Thermophoresis beyond Local Thermodynamic Equilibrium

Daniel B. Mayer,[1] Thomas Franosch,[1] Christof Mast,[2] and Dieter Braun[2,*]
[1]Institut für Theoretische Physik, Universität Innsbruck, Technikerstraße 21A, A-6020 Innsbruck, Austria
[2]Systems Biophysics, Physics Department, Nanosystems Initiative Munich and Center for NanoScience, Ludwig-Maximilians-Universität München, Amalienstrasse 54, D-80799 München, Germany

(Received 15 November 2021; accepted 8 March 2023; published 19 April 2023)

We measure the thermophoresis of polysterene beads over a wide range of temperature gradients and find a pronounced nonlinear phoretic characteristic. The transition to the nonlinear behavior is marked by a drastic slowing down of thermophoretic motion and is characterized by a Péclet number of order unity as corroborated for different particle sizes and salt concentrations. The data follow a single master curve covering the entire nonlinear regime for all system parameters upon proper rescaling of the temperature gradients with the Péclet number. For low thermal gradients, the thermal drift velocity follows a theoretical linear model relying on the local-equilibrium assumption, while linear theoretical approaches based on hydrodynamic stresses, ignoring fluctuations, predict significantly slower thermophoretic motion for steeper thermal gradients. Our findings suggest that thermophoresis is fluctuation dominated for small gradients and crosses over to a drift-dominated regime for larger Péclet numbers in striking contrast to electrophoresis.

DOI: 10.1103/PhysRevLett.130.168202

Molecules in solutions move along temperature gradients. This effect, termed thermophoresis or the Soret effect, was discovered about 150 years ago in aqueous solutions [1,2] and plays a key role in numerous fundamental problems and applications, including the separation of nonaqueous polymers [3], the geological movement of crude oil [4], oscillatory convection [5], convection in ferrofluids [6], polymer collapse [7,8], and even in plasma systems due to temperature gradients created by resonant plasmon excitations [9,10]. Thermophoresis of charged molecules such as RNA or DNA is comparably strong and therefore may constitute a fundamental element of the molecular evolution at the origin of life [11,12]. A strong focus lies on the aim to better understand and find geological nonequilibrium conditions in hydrothermal environments for the emergence of life [13,14]. Perhaps most importantly, thermophoresis has been employed to quantify biomolecule binding, termed microscale thermophoresis [15,16].

Yet, the description of thermophoresis strikes fundamental physical questions on the definition of thermodynamic equilibration and how it separates from nonequilibrium phenomena. Recently, the emergence of enhanced diffusion of self-heated particles [17] and the direct observation of hydrodynamic memory in Brownian motion [18] have both improved our understanding of diffusion processes and nonequilibrium phenomena [19,20]. In the recent past, thermophoresis has been approached within different theoretical linear models, choosing either a hydrodynamic [21–25] or thermodynamic viewpoint [26–29]. The former correctly incorporates dissipation via local fluid flow, however, it does not reflect the maximization of the number of microstates in the local thermodynamic equilibration of the counter ions in the Debye layer surrounding the particle [30]. For moderately charged molecules in water, the latter is the dominant effect and allows for a thermodynamic foundation of the Soret coefficient [31,32]. Both theoretical models for thermophoretic motion have been elaborated for the linear response, while the nonlinear regime has been virtually unexplored. Recent theoretical studies within a hydrodynamic approach [33,34] suggest that the observation of nonlinear effects in thermophoresis constitutes an experimental challenge.

Intuitively, one anticipates that the local-equilibrium assumption has to break down once the thermal gradients become strong and a regime of genuine nonequilibrium transport should emerge. Correspondingly, interesting questions arise, on what scale do such effects become relevant and how does thermophoresis evolve for even larger nonequilibrium driving? Does thermophoeretic motion become more efficient beyond the linear regime and what microscopic quantities determine the drift velocity? How can the breakdown of the local-equilibrium assumption be linked with approaches based on hydrodynamic stresses?

In this Letter, we explore the limit of local thermal equilibration by means of single-particle tracking to determine the thermal velocities of polystyrene beads (PSB) of several radii and different salt concentrations. Our measurements provide first experimental evidence for thermophoretic motion beyond local equilibrium, strikingly revealing the nonlinear regime, and pave the way to reconcile different theoretical approaches for linear response as limiting cases.

We have extended single-particle measurements of thermophoresis [31] by tracking fluorescent particles inside thin chambers as they move along an optically applied temperature gradient. The drift velocity is derived from the particle positions while the local temperature gradient is inferred from temperature-dependent fluorescence. This allows measuring the thermophoretic drift velocity and correlating it with the temperature gradient.

For small temperature gradients ∇T, the particle's motion strongly fluctuates while the overall thermophoretic effect becomes apparent only on larger length scales [see Fig. 1(a)]. In contrast, for larger thermal gradients the trajectory is strongly rectified and only small fluctuations are superimposed on the directed motion, as highlighted in Fig. 1(b). The crossover between the two regimes is expected once the timescale for diffusion processes becomes comparable to the timescale of thermophoretic motion. This insight suggests defining a dimensionless number $\mathrm{Pe} = \tau_{\mathrm{diff}}/\tau_{\mathrm{drift}}$, which we refer to as the (phoretic) Péclet number, by comparing the diffusion time $\tau_{\mathrm{diff}} = a^2/D$ to the thermophoretic-drift time $\tau_{\mathrm{drift}} = a/D_T|\nabla T|$. Correspondingly, for $\mathrm{Pe} \lesssim 1$ the movement of the particle is *fluctuation dominated*, while $\mathrm{Pe} \gtrsim 1$ describes the *drift-dominated* motion. Here a denotes the radius of the particle, D the diffusion coefficient, $D_T\nabla T$ is the drift velocity in linear response with the thermal diffusion coefficient D_T. Employing the definition of the Soret coefficient, $S_T = D_T/D$, the Péclet number simplifies to $\mathrm{Pe} = aS_T|\nabla T|$. Hence, the crossover $\mathrm{Pe} = 1$ occurs for thermal gradients

$$|\nabla T|_{\mathrm{c}} = (S_T a)^{-1}. \tag{1}$$

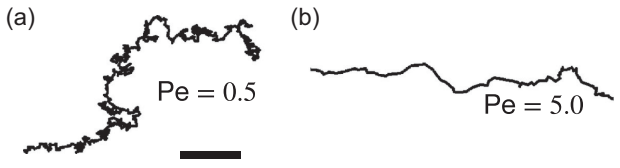

FIG. 1. Trajectories obtained from single-particle tracking of polystyrene beads (PSB) immersed in water for two different Péclet numbers (a) $\mathrm{Pe} = 0.5$ and (b) $\mathrm{Pe} = 5.0$. The scale bar corresponds to 20 μm. For $\mathrm{Pe} \lesssim 1$, the motion is dominated by diffusion and thermophoresis is rather slow. In contrast, for $\mathrm{Pe} \gtrsim 1$ hydrodynamic stresses become important, increasing the phoretic drift velocity.

The thermophoresis of polymers and molecules in solvents is experimentally well below this threshold. For example, single-stranded DNA with $a \approx 3$ nm and $S_T \approx 0.1\ \mathrm{K}^{-1}$ results in $|\nabla T|_{\mathrm{c}} \approx 3000\ \mathrm{K/\mu m}$, 5 orders of magnitude beyond the gradient $|\nabla T|^{\mathrm{exp}} \approx 0.05\ \mathrm{K/\mu m}$ used in the experiments. However, we could reach this regime for micrometer-sized polystyrene beads ($2a \gtrsim 1$ μm, $S_T \gtrsim 10\ \mathrm{K}^{-1}$) employing a special setup that created very steep thermal gradients $\gtrsim 0.1\ \mathrm{K/\mu m}$ (see Fig. S1e in Supplemental Material [35]). Considerable care had to be taken so that the particles were not influenced by possible artifacts from thermal convection, sedimentation, wall effects or optical trapping (see Supplemental Material [35]).

The strategy was to use 20 μm thin chambers, small enough to suppress thermal convection, but still 10 times larger than the largest particle. We created an optical warm spot by an IR heating laser and imaged the temperature distribution using thermosensitive fluorescent dyes [31,48] to quantify the temperature gradient.

Optical trapping was limited by keeping the heating laser defocused with a FWHM of 50 μm. We checked for possible experimental artifacts from trapping using heavy water as a solvent, which showed an eightfold reduced absorption of the laser light, leading to an equally reduced temperature gradient, while keeping optical trapping constant. In this case, no significant drift from optical trapping was observable [Figs. S1(d),1(e) in Supplemental Material [35]], demonstrating that optical trapping was not a distorting factor even for the largest particles.

As the particles move away from the center of the heated spot, the gradient becomes flatter and the velocity of the thermophoretic drift decreases. Measuring both the drift velocity and the thermal gradient independently as a function of the distance to the heating spot allows testing the linearity of the thermophoretic drift relation

$$\mathbf{U} = -D_T\nabla T. \tag{2}$$

We compare our experimental findings to the linear theoretical prediction for the drift velocities [Eq. (2)]. To this end we combine two linear theoretical approaches for the thermophoretic motion of a single charged colloid. The first is derived within irreversible thermodynamics and is expected to be valid at local thermodynamic equilibrium conditions [32] (see also Supplemental Material [35]) for $\mathrm{Pe} \lesssim 1$. The second model treats the solvent surrounding the particle as a continuous medium [49,50] (see also Supplemental Material [35]) subject to local hydrodynamic stresses causing fluid flow and hence directed particle motion in response to a temperature gradient. Here the detailed double-layer deformation is accounted for, based on field equations for hydrodynamic flow, local electric fields, and ion concentrations within linear response theory. The hydrodynamic approach in linear response is expected to be valid for all experimentally accessible temperature

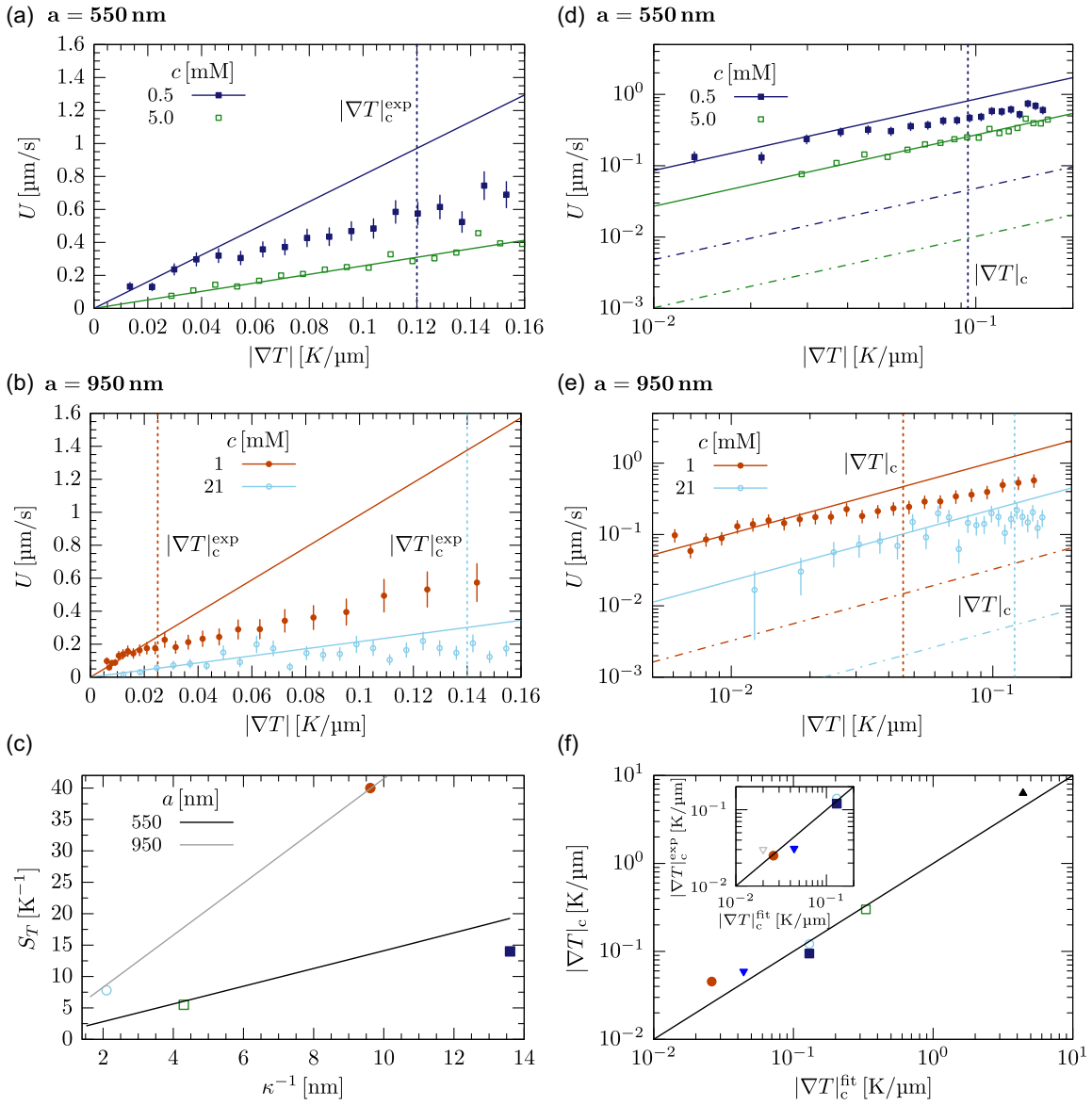

FIG. 2. Linear fits to the experimental measurements (symbols) for radii (a) $a = 550$ and (b) $a = 950$ nm and for different salt concentrations c. The crossover temperature gradients $|\nabla T|_c^{\mathrm{exp}}$ where the calculated velocities deviate by 70% from the linear drift relation are indicated by the vertical dashed lines. (c) Soret coefficient S_T vs Debye length κ^{-1}. Full lines correspond to the theoretical predictions [see Eq. (4) in the Supplemental Material [35]]. (d),(e) Comparison to the different linear-theoretical-model predictions for the same radii and concentrations. Vertical dashed lines represent the crossover temperature gradient $|\nabla T|_c$ obtained from theory (see Table S1 in Supplemental Material [35]). Full lines denote results from both the thermodynamic and hydrodynamic approach by superimposing the corresponding thermophoretic drift velocities. Dashed-dotted lines are solutions within a hydrodynamic viewpoint. (f) Scatter plot of the crossover temperature gradient $|\nabla T|_c^{\mathrm{fit}}$ obtained from linearly fitting the data according to Eq. (2) vs $|\nabla T|_c$. Inset: Same for the experimentally determined thermal gradient $|\nabla T|_c^{\mathrm{exp}}$ (see Table S1 in the Supplemental Material [35]).

gradients since the relative temperature variations $a|\nabla T|/T \approx 10^{-3} - 10^{-4} \ll 1$ are small over the particle radius a for ambient temperature $T \approx 300$ K and temperature gradients $|\nabla T| \lesssim 0.2$ K/μm (see Table S1 in Supplemental Material [35]). Here we suggest that for $\mathrm{Pe} \lesssim 1$ the thermal diffusion coefficient consists of two contributions $D_T = D_T^{\mathrm{hyd}} + D_T^{\mathrm{eq}}$ superimposed by linearity with D_T^{hyd} from hydrodynamic theory, and D_T^{eq} from local thermodynamic equilibrium. As the temperature gradient reaches the crossover value of Eq. (1), we expect a slowing down of the drift velocity due to the breakdown of the Brownian motion contribution to thermophoresis, the dominating term for micrometer-sized particles.

We formally define an *effective* thermal diffusion coefficient $D_T^{\mathrm{eff}} := U/|\nabla T|$ (with $U = |\mathbf{U}|$) which depends on the thermal gradient and incorporates implicitly all nonlinear effects in the temperature gradient. For small $\mathrm{Pe} \lesssim 1$ it reduces to the linear response value D_T^{eq} while for large

gradients Pe $\gg 1$ it is expected to converge to $D_T^{\mathrm{eff}} \approx D_T^{\mathrm{hyd}}$ with $D_T^{\mathrm{hyd}} \ll D_T^{\mathrm{eq}}$. Clearly, the inherently linear hydrodynamic theory cannot account for the nonlinear crossover. Nevertheless, it is anticipated to predict the strong decrease in the amplitude of the thermal velocities U.

We performed the drift experiment for two PSB radii and two Soret coefficients, tuned by enhancing the salt concentrations and thus the Debye length [Table S1 in Supplemental Material [35] and Figs. 2(b) and 2(c)]. The thermophoretic mobilities D_T can be fitted for Pe $\lesssim 1$ (see Table S1 in [35]) since there linearity in the gradient [Eq. (2)] holds. The corresponding Soret coefficients $S_T = D_T/D$ follow the theoretical predictions [32,50] quantitatively [Fig. 2(c)] with an effective surface charge density of $-4500\ e\ \mu\mathrm{m}^{-2}$ that was determined from electrophoresis of particles with a radius of 20 nm with identical surface modifications [31]. This confirms a previously observed linear dependence on Debye length and a quadratic dependence on particle size for low salt concentrations [31,32]. However, there are deviations from this linear relation [Eq. (2)], marked vertically in the plots [Figs. 2(b) and 2(c)], where we define the threshold thermal gradient $|\nabla T|_{\mathrm{c}}^{\mathrm{exp}}$ for a chosen deviation of 70% from the linear behavior. This choice is a compromise to account for a steep thermal gradient and measure particles with a high S_T while minimizing experimental uncertainties for the smaller ones. As can be inferred from Fig. 2(f) (inset) the threshold matches the expectation of Eq. (1) for the two PSB radii and different salt concentrations. We also compare the experimentally obtained values for the drift velocities with the theoretical linear predictions and find good agreement for Pe $\lesssim 1$ [Figs. 2(d) and 2(e)].

The slowing down is consistent with the linear hydrodynamic model [49,50] (and Supplemental Material [35]), see Figs. 2(e) and 2(f) (dashed-dotted lines), as well as with a similar recent theoretical approach [22], predicting up to 20 times lower drift velocities. Furthermore the crossover thermal gradient $|\nabla T|_c$ obtained from the linear theoretical model (SM [35]) is in accordance with the calculated threshold $|\nabla T|_c^{\mathrm{fit}}$, as well as the experimentally obtained $|\nabla T|_{\mathrm{c}}^{\mathrm{exp}}$, see Fig. 2(f) corroborating consistency between the different criteria for the crossover gradient.

Having pinpointed the relevant crossover thermal gradient, we employ the linear response prediction to identify the characteristic velocity scale $D_T|\nabla T|_c = D_T(S_T a)^{-1} = D/a$. Then we plot the rescaled velocity Ua/D vs the rescaled temperature gradient $|\nabla T|/|\nabla T|_c = \mathrm{Pe}$ and find data collapse for rescaled temperature gradients varying over almost 3 orders of magnitude and 2 decades for the drift velocities, see Fig. 3. The crossover to a pronounced nonlinear regime appears to be universal irrespective of the salt concentration or particle radii. Experimental artifacts from thermal convection and sedimentation prevent measurements with even larger thermal gradients or using larger particles to fully observe the transition.

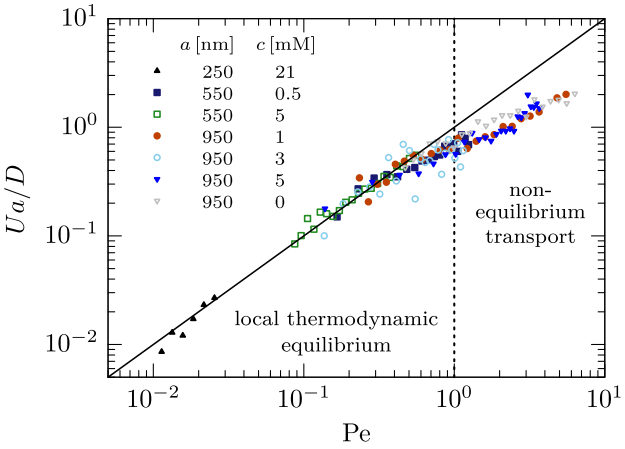

FIG. 3. Single master curve with pronounced nonlinear deviations setting in around Pe $\gtrsim 1$ for all particle radii and salt concentrations (see also Table S1 in Supplemental Material [35]).

Conclusion.—We have measured the thermophoretic motion for micrometer-sized colloidal particles for an extensive range of Péclet numbers and find good agreement with a model based on local thermodynamic equilibrium for small temperature gradients, while for larger Péclet numbers the drift velocity becomes sublinear. The data collapse for the linear and nonlinear response for all radii and salt concentrations corroborates a universal underlying mechanism for the transition from local thermodynamic equilibrium to a genuine nonequilibrium state.

Based on our measurements, we argue that since Pe $\ll 1$ for typical measurements in solution, local equilibrium should be assumed and the thermophoretic motion is fluctuation dominated. Only for the large Péclet numbers achieved in our experiments, thermophoresis becomes drift dominated and approaches the hydrodynamic model. This observation suggests that thermophoresis is inherently different from electrophoresis where typically the electrophoretic drift velocity $U^{\mathrm{el}} \gtrsim D/a$ such that the motion is drift dominated and is well described within a hydrodynamic approach [51–54].

We are grateful to Werner Köhler, Alois Würger, and Jan Dhont for various discussions. We thank Stefan Duhr for help in the experiments. We thank Ingmar Schoen for help in the sedimentation profile, Michael Haslauer and Maren Reichl for assistance with the thermophoresis experiments and Alexandra Kühnlein and Patrick Kudella for corrections on the manuscript. The theoretical part (D. B. M., T. F.) was supported by the Austrian Science Fund (FWF): I5257-N. For the experimental part (C. M., D. B.), we gratefully acknowledge support from the Deutsche Forschungsgemeinschaft (SFB 1032 Project A04), the CRC 235 Project P07 (Project-ID 364653263), the European Research Council ERC Evotrap (Grant No. 787356 D. B.) and a grant from the Simons Foundation (SCOL 327125).

*To whom correspondence should be addressed.
dieter.braun@lmu.de

[1] C. Soret, Sur l'état d'équilibre que prend, au point de vue de sa concentration, une dissolution saline primitivement homogène, dont deux parties sont portées à des températures différentes; Archives de Genève, 3e periode, t. II, p. 48; 1879, J. Phys. Theor. Appl. **9**, 331 (1879).
[2] C. Ludwig, Diffusion zwischen ungleich erwärmten Orten gleich zusammengesetzer Lösung, Sitzunbsberichte der mathematisch-naturwissenschaftlichen Classe der Kaiserlichen Akademie der Wissenschaften Wien **20** (1856).
[3] M. E. Hovingh, G. H. Thompson, and J. C. Giddings, Column parameters in thermal field-flow fractionation, Anal. Chem. **42**, 195 (1970).
[4] P. Georis, F. Montel, S. Van Vaerenbergh, Y. Decroly, and J. C. Legros, Measurement of the Soret coefficient in crude oil, Eur. Pet. Conf. (1998).10.2118/50573-MS
[5] D. Jung and M. Lücke, Localized Waves Without the Existence of Extended Waves: Oscillatory Convection of Binary Mixtures with Strong Soret Effect, Phys. Rev. Lett. **89**, 054502 (2002).
[6] E. Blums, S. Odenbach, A. Mezulis, and M. Maiorov, Soret coefficient of nanoparticles in ferrofluids in the presence of a magnetic field, Phys. Fluids **10**, 2155 (1998).
[7] R. Kita and S. Wiegand, Soret coefficient of poly(N-isopropylacrylamide)/water in the vicinity of coil-globule transition temperature, Macromolecules **38**, 4554 (2005).
[8] M. Wolff, D. Braun, and M. A. Nash, Detection of thermoresponsive polymer phase transition in dilute low-volume format by microscale thermophoretic depletion, Anal. Chem. **86**, 6797 (2014).
[9] S. Simoncelli, J. Summer, S. Nedev, P. Kühler, and J. Feldmann, Combined optical and chemical control of a microsized photofueled Janus particle, Small **12**, 2854 (2016).
[10] F. Nicoli, D. Verschueren, M. Klein, C. Dekker, and M. P. Jonsson, DNA translocations through solid-state plasmonic nanopores, Nano Lett. **14**, 6917 (2014).
[11] D. Niether, D. Afanasenkau, J. K. G. Dhont, and S. Wiegand, Accumulation of formamide in hydrothermal pores to form prebiotic nucleobases, Proc. Natl. Acad. Sci. U.S.A. **113**, 4272 (2016).
[12] C. B. Mast, S. Schink, U. Gerland, and D. Braun, Escalation of polymerization in a thermal gradient, Proc. Natl. Acad. Sci. U.S.A. **110**, 8030 (2013).
[13] N. Goldenfeld, T. Biancalani, and F. Jafarpour, Universal biology and the statistical mechanics of early life, Phil. Trans. R. Soc. A **375**, 20160341 (2017).
[14] F. Jafarpour, T. Biancalani, and N. Goldenfeld, Noise-Induced Mechanism for Biological Homochirality of Early Life Self-Replicators, Phys. Rev. Lett. **115**, 158101 (2015).
[15] C. J. Wienken, P. Baaske, U. Rothauer, D. Braun, and S. Duhr, Protein-binding assays in biological liquids using microscale thermophoresis, Nat. Commun. **1** (2010).
[16] M. Jerabek-Willemsen, C. J. Wienken, D. Braun, P. Baaske, and S. Duhr, Molecular interaction studies using microscale thermophoresis, Assay Drug Dev. Technol. **9**, 342 (2011).
[17] D. Rings, R. Schachoff, M. Selmke, F. Cichos, and K. Kroy, Hot Brownian Motion, Phys. Rev. Lett. **105**, 090604 (2010).
[18] T. Franosch, M. Grimm, M. Belushkin, F. M. Mor, G. Foffi, L. Forró, and J. S., Resonances arising from hydrodynamic memory in Brownian motion, Nature (London) **478**, 85 (2011).
[19] E. Fodor, C. Nardini, M. E. Cates, J. Tailleur, P. Visco, and F. van Wijland, How Far from Equilibrium is Active Matter?, Phys. Rev. Lett. **117**, 038103 (2016).
[20] C. Battle, C. P. Broedersz, N. Fakhri, V. F. Geyer, J. Howard, C. F. Schmidt, and F. C. MacKintosh, Broken detailed balance at mesoscopic scales in active biological systems, Science **352**, 604 (2016).
[21] J. Burelbach, D. Frenkel, I. Pagonabarraga, and E. Eiser, A unified description of colloidal thermophoresis, Eur. Phys. J. E **41**, 7 (2018).
[22] J. Burelbach and H. Stark, Determing phoretic mobilities with Onsager's reciprocal relations: Electro- and thermophoresis revisited, Eur. Phys. J. E **42**, 4 (2019).
[23] S. Fayolle, T. Bickel, and A. Würger, Thermophoresis of charged colloidal particles, Phys. Rev. E **77**, 041404 (2008).
[24] A. Parola and R. Piazza, Particle thermophoresis in liquids, Eur. Phys. J. E **15**, 255 (2004).
[25] E. Ruckenstein, Can phoretic motions be treated as interfacial tension gradient driven phenomena?, J. Colloid Interface Sci. **83**, 77 (1981).
[26] A. Würger, Is Soret equilibrium a non-equilibrium effect?, C.R. Méc. **341**, 438 (2013).
[27] N. Kocherginsky and M. Gruebele, Thermodiffusion: The physico-chemical mechanics view, J. Chem. Phys. **154**, 024112 (2021).
[28] E. Bringuier and A. Bourdon, Colloid transport in nonuniform temperature, Phys. Rev. E **67**, 011404 (2003).
[29] S. R. De Groot and P. Mazur, *Non-Equilibrium Thermodynamics* (Dover Publications, New York, 1969).
[30] S. Duhr and D. Braun, Thermophoretic Depletion Follows Boltzmann Distribution, Phys. Rev. Lett. **96**, 168301 (2006).
[31] S. Duhr and D. Braun, Why molecules move along a temperature gradient, Proc. Natl. Acad. Sci. U.S.A. **103**, 19678 (2006).
[32] J. K. G. Dhont, S. Wiegand, S. Duhr, and D. Braun, Thermodiffusion of charged colloids: Single-particle diffusion, Langmuir **23**, 1674 (2007).
[33] H. Sugioka, Nonlinear thermokinetic phenomena due to the Seebeck effect, Langmuir **30**, 8621 (2014).
[34] H. Sugioka, Direct simulation on nonlinear thermokinetic phenomena due to induced-charge electroosmosis, J. Fluid Mech. **855**, 736 (2018).
[35] See Supplemental Material at http://link.aps.org/supplemental/10.1103/PhysRevLett.130.168202 which includes Refs. [36–47] for further details regarding the experimental method, the theoretical model, and further calculations.
[36] S. Duhr, S. Arduini, and D. Braun, Thermophoresis of DNA determined by microfluidic flourescence, Eur. Phys. J. E **15**, 277 (2004).
[37] D. Braun, N. L. Goddard, and A. Libchaber, Exponential DNA Replication by Laminar Convection, Phys. Rev. Lett. **91**, 158103 (2003).
[38] A. Würger, Transport in Charged Colloids Driven by Thermoelectricity, Phys. Rev. Lett. **101**, 108302 (2008).

[39] P. Baaske, S. Duhr, and D. Braun, Melting curve analysis in a snapshot, Appl. Phys. Lett. **91**, 133901 (2007).
[40] M. L. Cordero, E. Verneuil, F. Gallaire, and C. N. Baroud, Time-resolved temperature rise in a thin liquid film due to laser absorption, Phys. Rev. E **79**, 011201 (2009).
[41] T. Tlusty, A. Meller, and R. Bar-Ziv, Optical Gradient Forces of Strongly Localized Fields, Phys. Rev. Lett. **81**, 1738 (1998).
[42] M. Ichikawa, H. Ichikawa, K. Yoshikawa, and Y. Kimura, Extension of a DNA Molecule by Local Heating with a Laser, Phys. Rev. Lett. **99**, 148104 (2007).
[43] N. Fuson, H. M. Randall, and D. M. Dennison, The far infra-red absorption spectrum and the rotational structure of the heavy water vapor molecule, Phys. Rev. **56**, 982 (1939).
[44] J. K. G. Dhont and W. J. Briels, Single-particle thermal diffusion of charged colloids: Double-layer theory in a temperature gradient, Eur. Phys. J. E **25**, 61 (2008).
[45] J. N. Agar, C. Y. Mou, and J. L. Lin, Single-ion heat of transport in electrolyte solutions: a hydrodynamic theory, J. Phys. Chem. **93**, 2079 (1989).
[46] L. D. Landau, E. M. Lifshitz, L. P. Pitaevskii, J. S. Bell, M. J. Kearsley, and J. B. Sykes, *Electrodynamics of Continuous Media* (Elsevier, New York, 2013), Vol. 8.
[47] A. S. Khair and T. M. Squires, The influence of hydrodynamic slip on the electrophoretic mobility of a spherical colloidal particle, Phys. Fluids **21**, 042001 (2009).
[48] J. Chan, J. J. Popov, S. Kolisnek-Kehl, and D. G. Least, Soret coefficients for aqueous polyethylene glycol solutions and some tests of the segmental model of polymer thermal diffusion, J. Solution Chem. **32**, 197 (2003).
[49] S. N. Rasuli and R. Golestanian, Soret Motion of a Charged Spherical Colloid, Phys. Rev. Lett. **101**, 108301 (2008).
[50] D. B. Mayer, D. Braun, and T. Franosch, companion paper, Thermophoretic motion of a charged single colloidal particle, Phys. Rev. E **107**, 044602 (2023).
[51] O. A. Hickey, T. N. Shendruk, J. L. Harden, and G. W. Slater, Simulations of Free-Solution Electrophoresis of Polyelectrolytes with a Finite DEbye Length Using the Debye-Hückel Approximation, Phys. Rev. Lett. **109**, 098302 (2012).
[52] K. Grass, U. Böhme, U. Scheler, H. Cottet, and C. Holm, Importance of Hydrodynamic Shielding for the Dynamic Behavior of Short Polyelectrolyte Chains, Phys. Rev. Lett. **100**, 096104 (2008).
[53] R. W. O'Brien and L. R. White, Electrophoretic mobility of a spherical colloidal particle, J. Chem. Soc., Faraday Trans. 2 **74**, 1607 (1978).
[54] H. Ohshima, Electrophoresis of soft particles, Adv. Colloid Interface Sci. **62**, 189 (1995).